Electronic Supplementary Material (ESI) for Journal of Materials Chemistry A.
This journal is © The Royal Society of Chemistry 2019

Electronic Supporting Information for

Modulating Charge Transfer Dynamics for g-C_3N_4 through Dimension and Interface Engineered Transition Metal Phosphide co-catalyst for Efficient Visible-Light Photocatalytic Hydrogen Generation

Fu Zhang,[a] Jihua Zhang,[b] Jianmin Li,[c] Xu Jin,[c] Yapeng Li,[a] Min Wu,[d] Xiongwu Kang,[d] Tao Hu,[e] Xiaoqi Wang,[c] Wei Ren[e] and Genqiang Zhang*[a]

[a] Division of Nanomaterials & Chemistry, Hefei National Research Center for Physical Sciences at the Microscale, Department of Materials Science and Engineering, University of Science and Technology of China, Hefei 230026, China

[b] Guizhou Provincial Key Laboratory of Computational Nano-Material Science, Guizhou Education University, Guiyang 550018, China

[c] Research Institute of Petroleum Exploration & Development (RIPED), PetroChina, No. 20 Xueyuan Road, Haidian District, Beijing, 100083, P. R. China

[d] New Energy Research Institute, College of Environment and Energy, South China University of Technology, Guangzhou Higher Education Mega Centre, Guangzhou 510006, China

[e] International Centre for Quantum and Molecular Structures, Physics Department, Shanghai University, Shanghai 200444, China

Corresponding Author:

G. Q. Zhang, E-mail: gqzhangmse@ustc.edu.cn

Figures

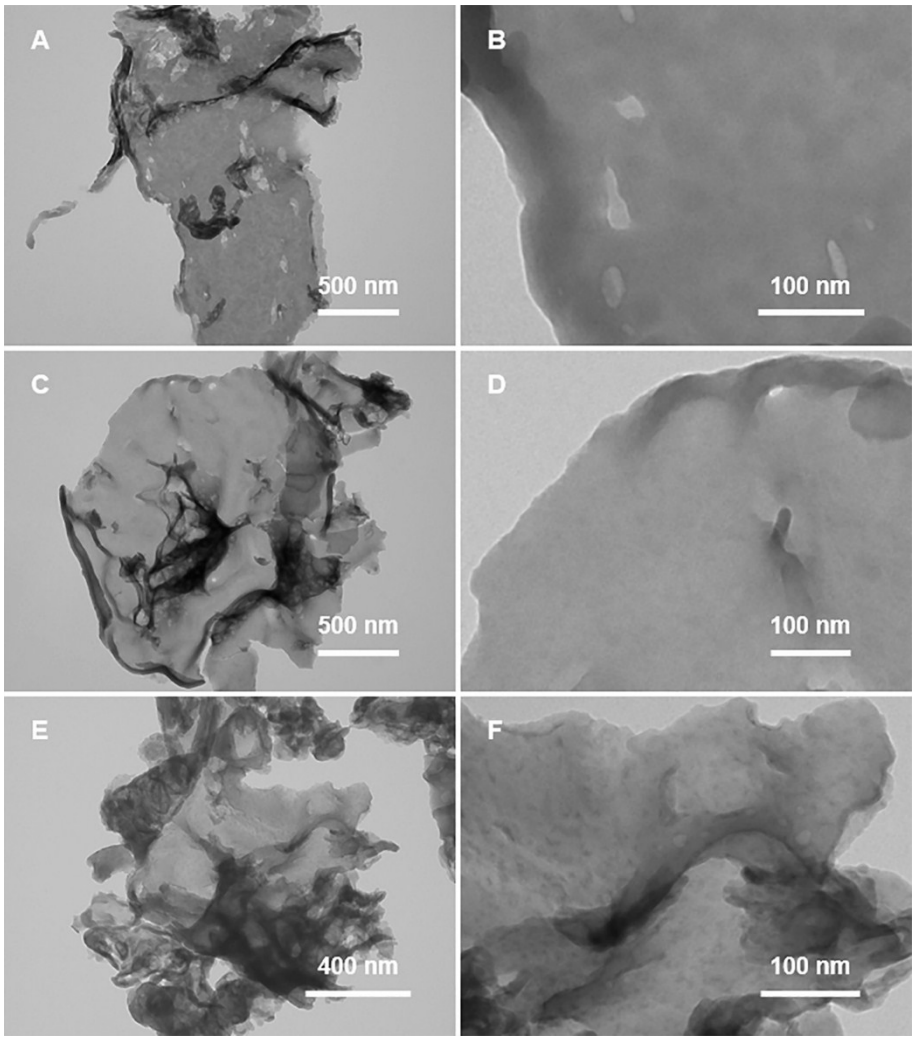

Fig. S1 Low-magnification and high-magnification TEM images of (A, B) pure g-C_3N_4, (C, D) Co-glycolate/g-C_3N_4 composites and (E, F) the 2.5CP/CN sample.

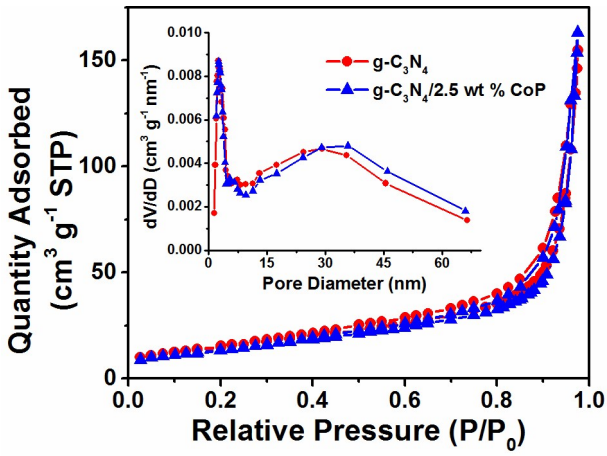

Fig. S2 Nitrogen adsorption-desorption isotherms and the corresponding pore size distribution curves (inset) of g-C_3N_4 and 2.5CP/CN samples.

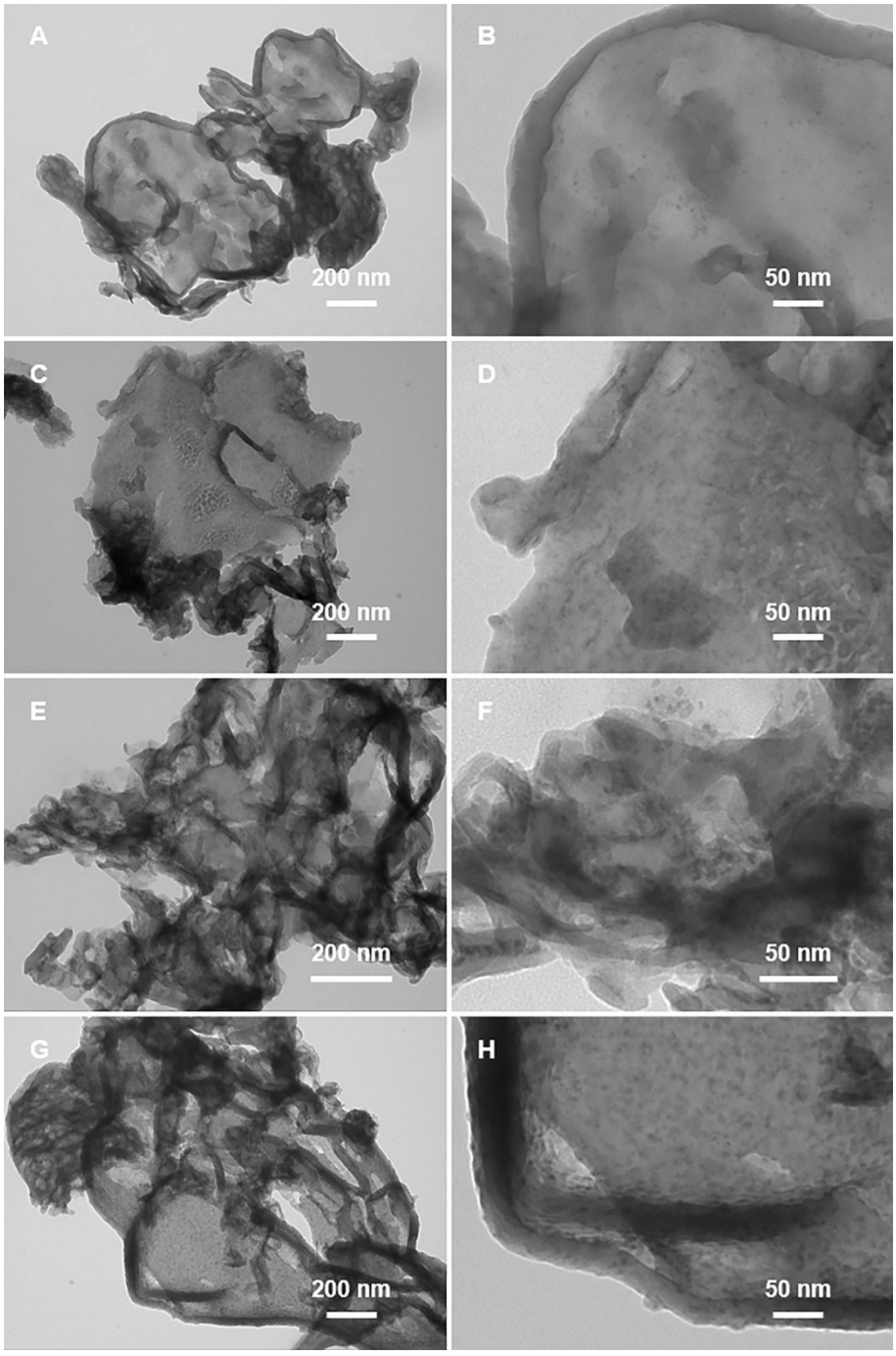

Fig. S3 Low-magnification and high-magnification TEM images of (A, B) 1.25CP/CN, (C, D) 5CP/CN, (E, F) 7.5CP/CN and (G, H) 10CP/CN.

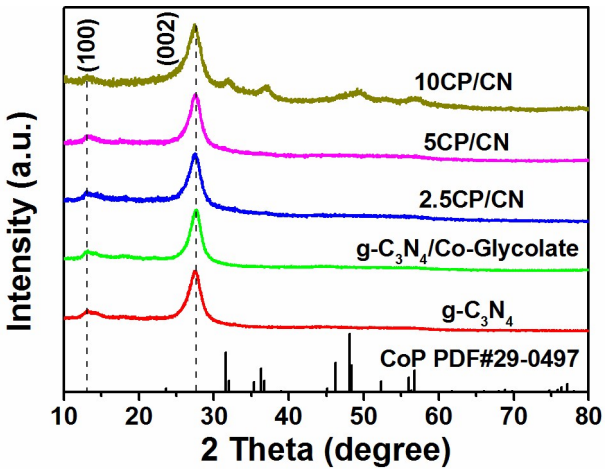

Fig. S4 XRD patterns of the pure g-C_3N_4, Co-Glycolate/g-C_3N_4, CoP/g-C_3N_4 composites with variable CoP mass contents (2.5, 5, 10 wt%).

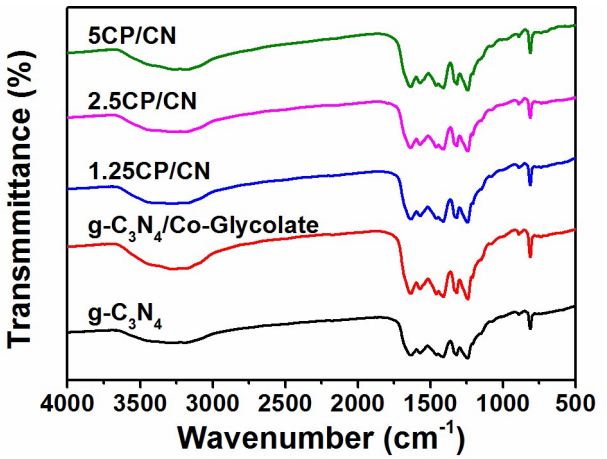

Fig. S5 FT-IR spectra of the pure g-C_3N_4, Co-Glycolate/g-C_3N_4, CoP/g-C_3N_4 composites with variable CoP mass contents (1.25, 2.5, 5 wt%).

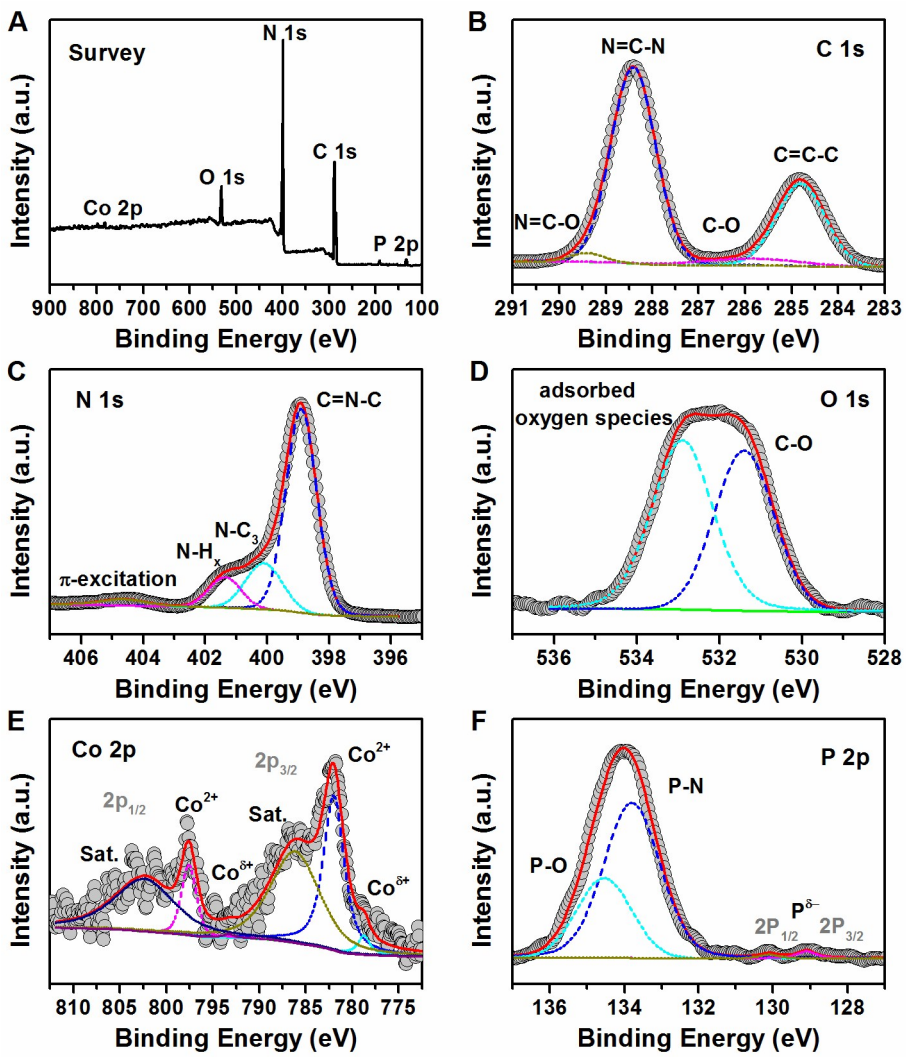

Fig. S6 XPS spectra for 2.5CP/CN sample.

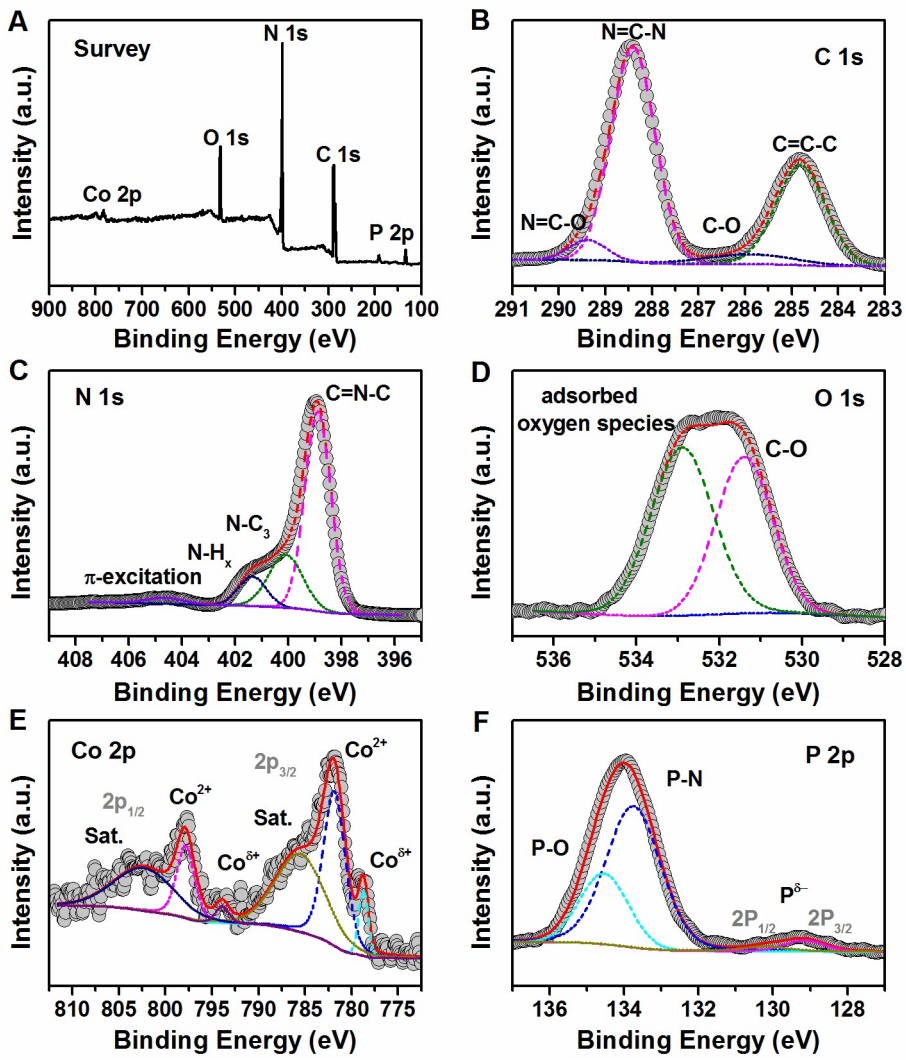

Fig. S7 High resolution XPS results of 7.5CP/CN sample.

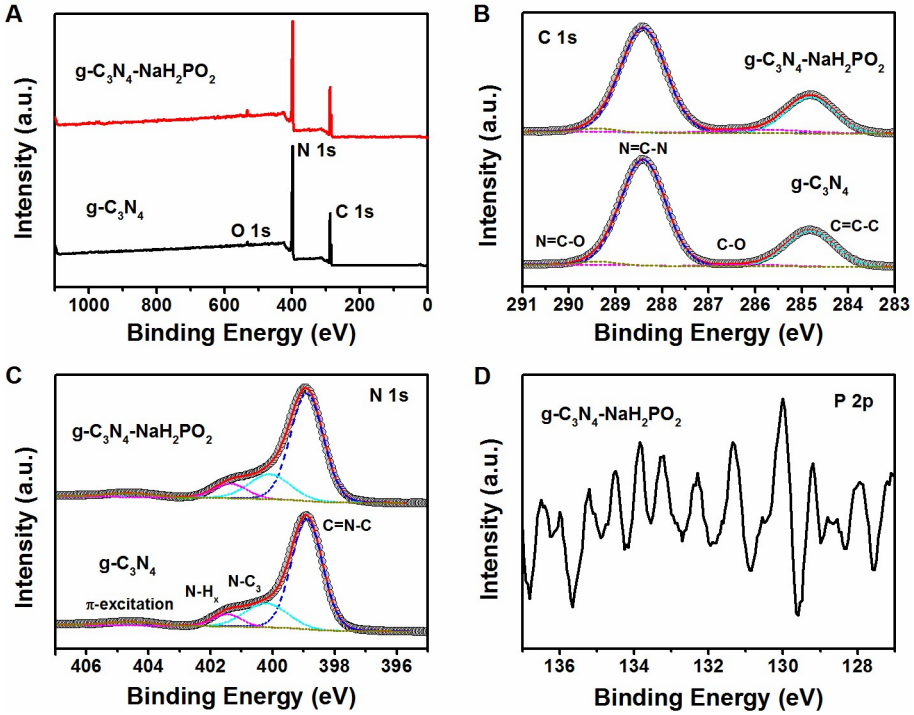

Fig. S8 XPS spectra for pristine g-C_3N_4 and g-C_3N_4 after heated with NaH_2PO_2.

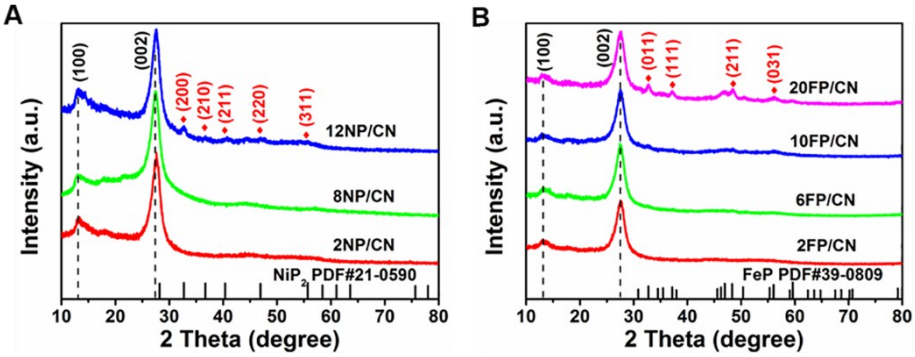

Fig. S9 XRD patterns of (A) the NiP_2/g-C_3N_4 composites with variable NiP_2 mass contents (2, 8, 12 wt%) and (B) the FeP/g-C_3N_4 composites with variable FeP mass contents (2, 6, 10, 20 wt%).

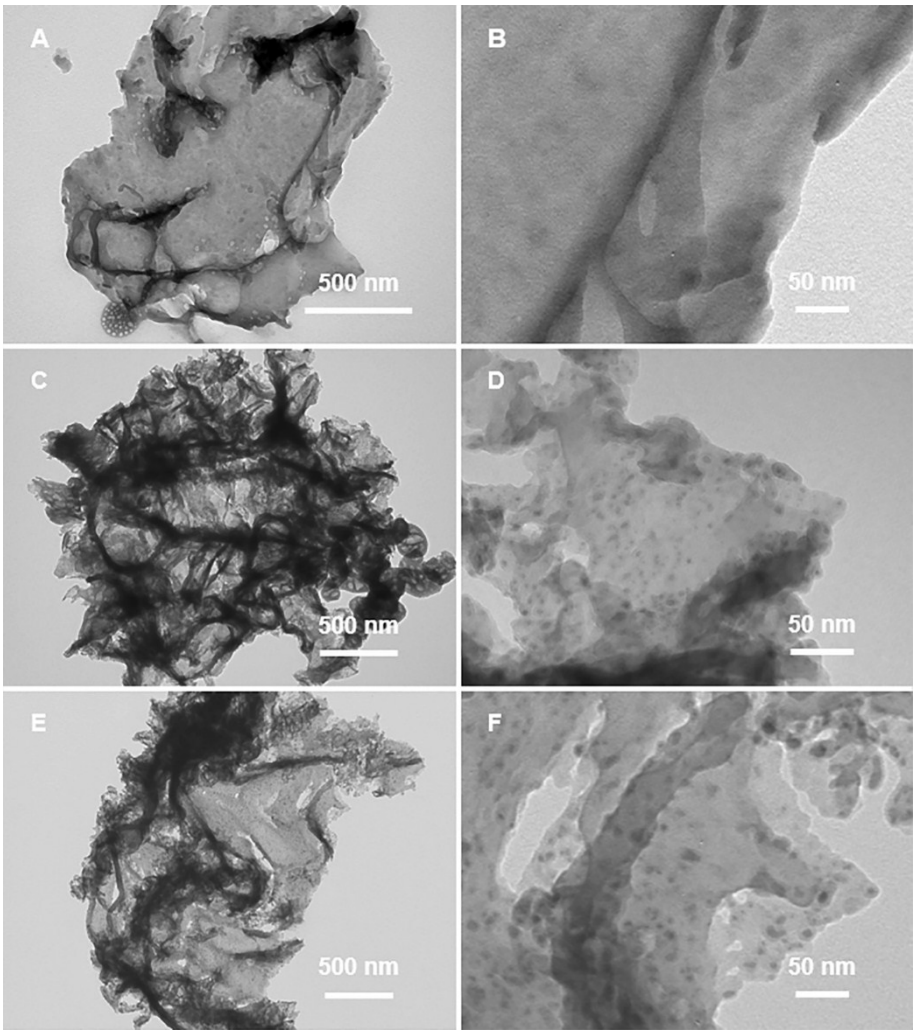

Fig. S10 Low-magnification and high-magnification TEM images of (A, B) 2 wt% NiP_2/g-C_3N_4, (C, D) 8 wt% NiP_2/g-C_3N_4 and (E, F) 12 wt% NiP_2/g-C_3N_4.

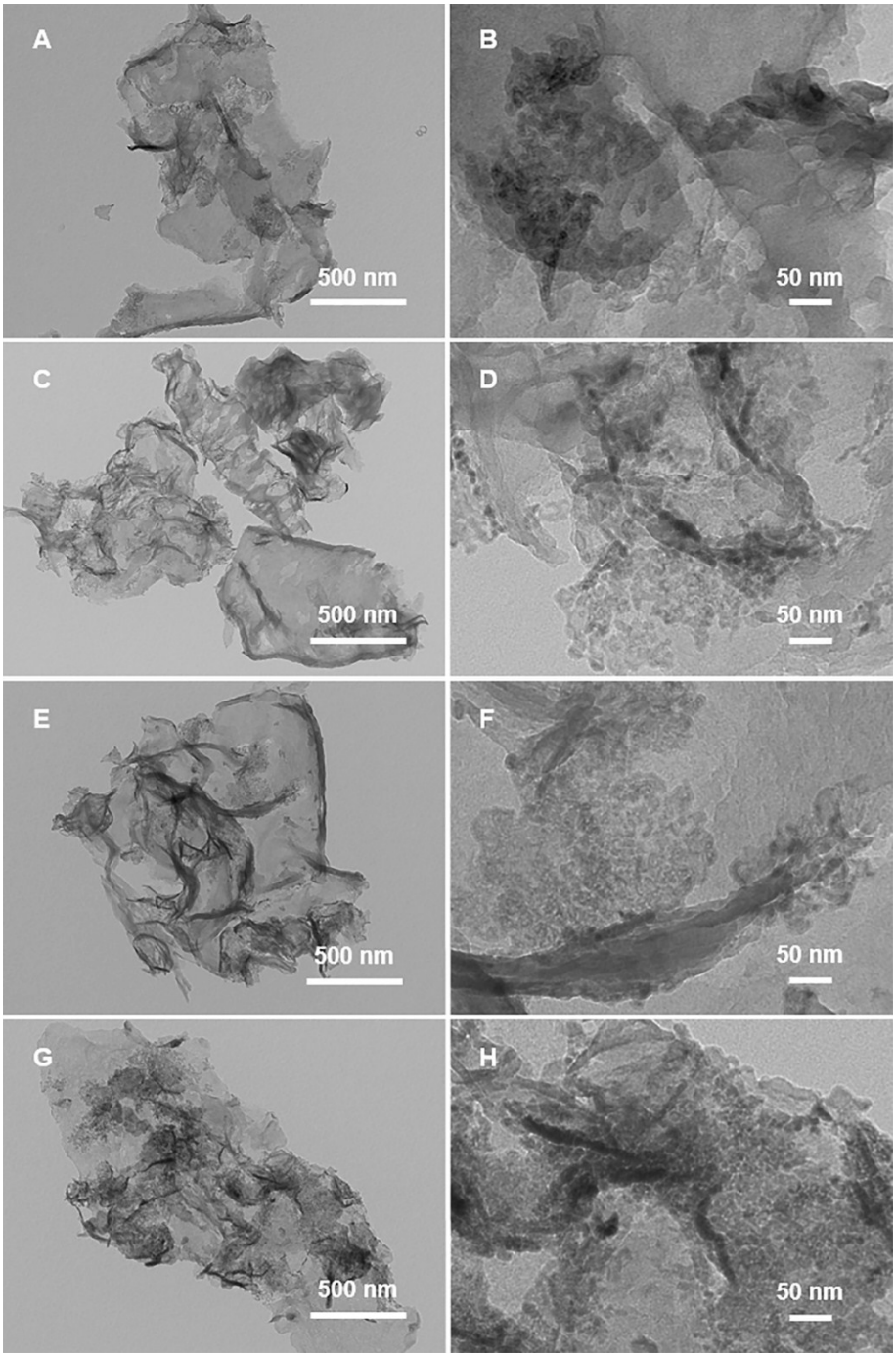

Fig. S11 Low-magnification and high-magnification TEM images of (A, B) 2 wt% FeP/g-C_3N_4, (C, D) 6 wt% FeP/g-C_3N_4, (E, F) 10 wt% FeP/g-C_3N_4 and (G, H) 20 wt% FeP/g-C_3N_4.

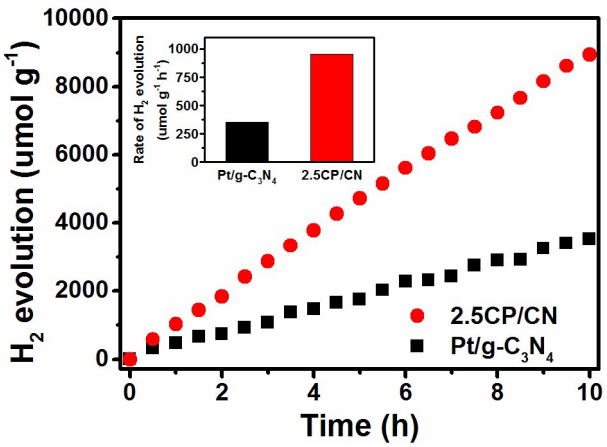

Fig. S12 Time course of photocatalytic H_2 production for 2.5 wt% Pt/g-C_3N_4 and 2.5CP/CN samples under visible light irradiation (λ > 420 nm) from 300 W Xe lamp using TEOA as the sacrificial agent.

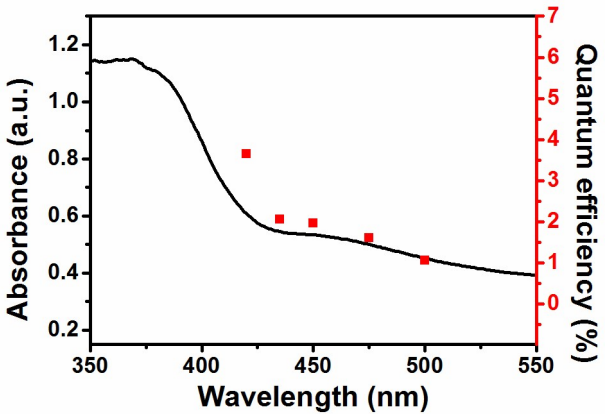

Fig. S13 The UV-vis diffuse spectrum (left axis) and wavelength-dependent quantum efficiency (right axis) of 2.5CP/CN for H_2 evolution (irradiation by a 300 W Xe lamp using a band-pass filter of full width at half maximum (FWHM) = 15 nm).

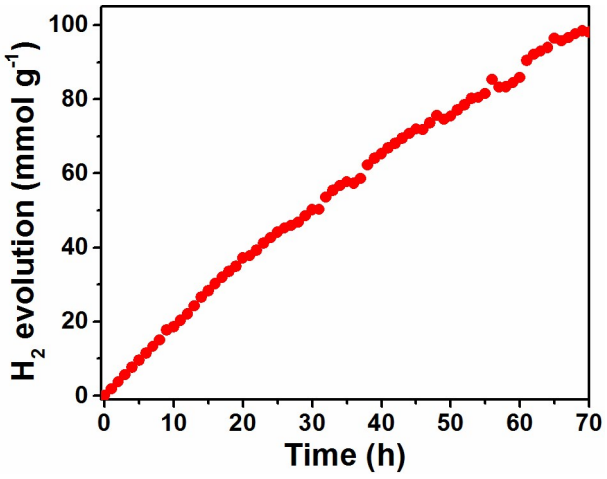

Fig. S14 Long-term photocatalytic H_2 evolution with 2.5CP/CN sample under simulated solar irradiation (λ > 300 nm) from 300 W Xe lamp using TEOA as the sacrificial agent.

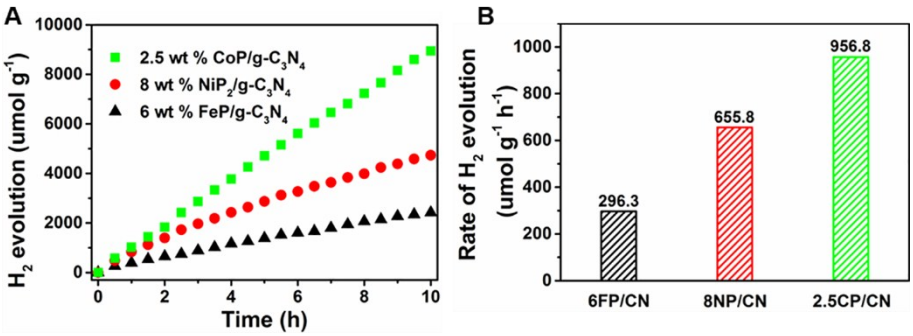

Fig. S15 (A) Time courses of photocatalytic H_2 evolution and (B) photocatalytic H_2 evolution rates over 2.5 wt% CoP/g-C_3N_4/, 8 wt% NiP_2/g-C_3N_4 and 6 wt% FeP/g-C_3N_4 hybrid photocatalysts in 10 vol% triethanolamine (TEOA) aqueous solution under visible light irradiation (λ > 420 nm).

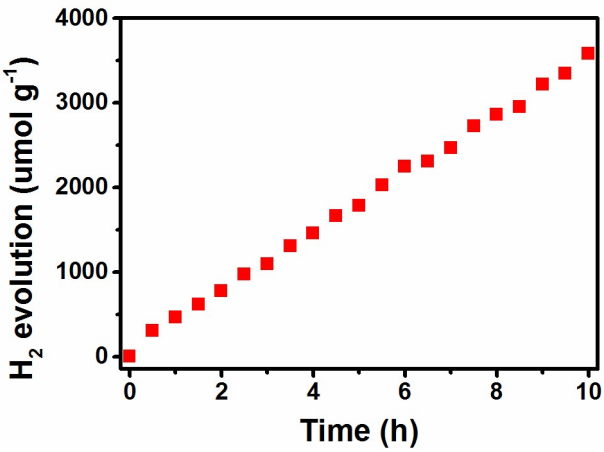

Fig. S16 Time course of H_2 production for 2.5 wt% Pt/g-C_3N_4-NaH_2PO_2 sample under visible light irradiation (λ > 420 nm) from 300 W Xe lamp using TEOA as the sacrificial agent.

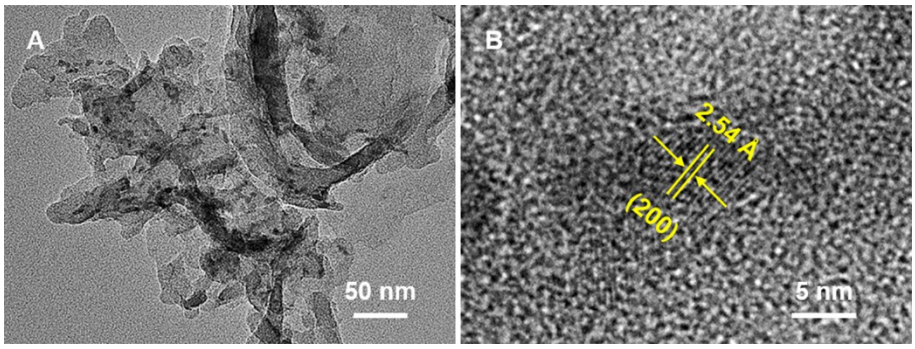

Fig. S17 TEM images of 2.5CP/CN sample after 70 h of continuous photocatalytic hydrogen production.

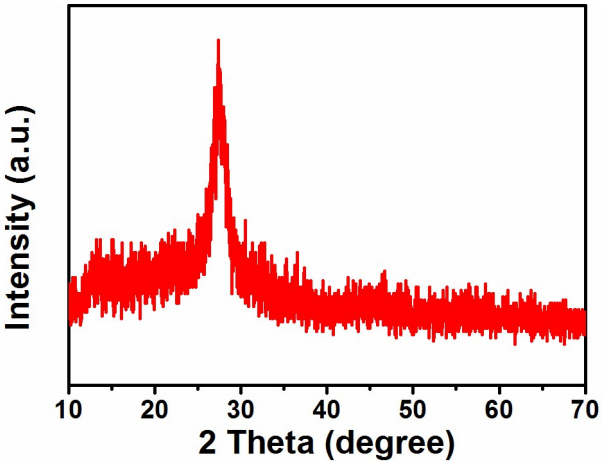

Fig. S18 XRD pattern of 2.5CP/CN sample after 70 h of continuous photocatalytic hydrogen production.

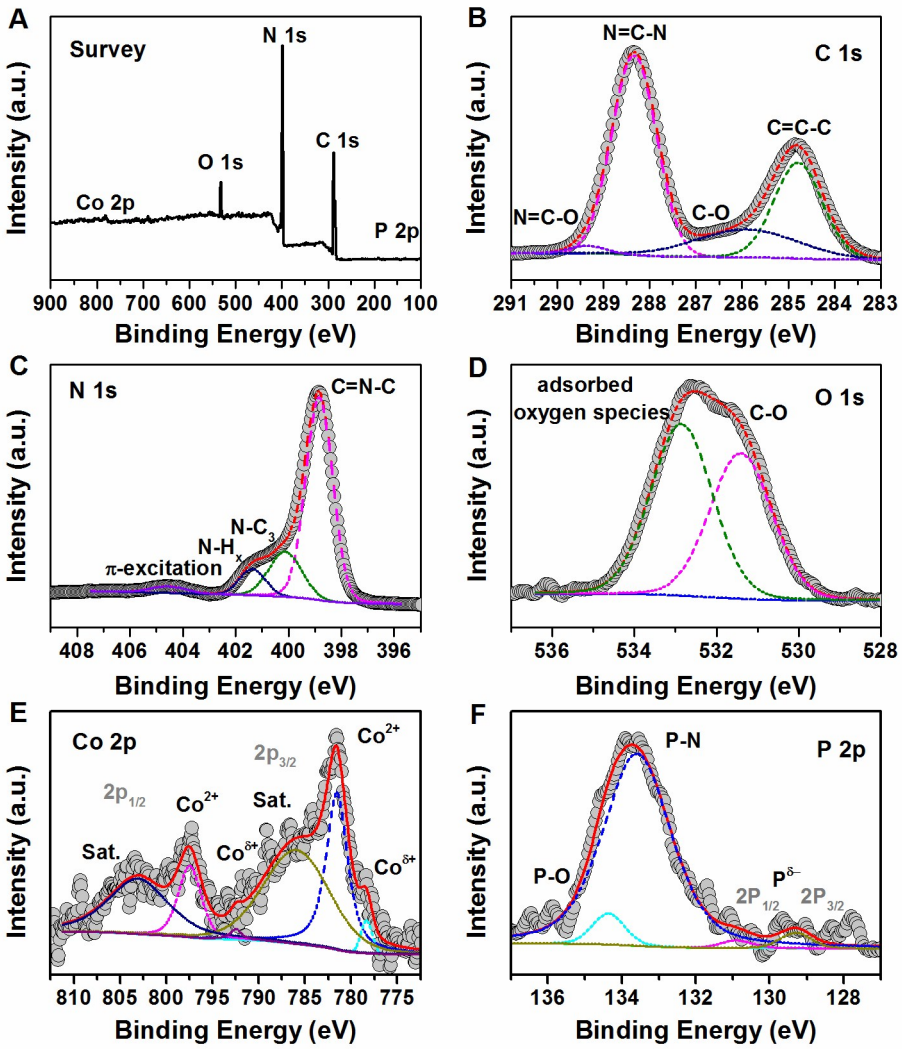

Fig. S19 (A) Co 2p and (B) P 2p XPS survey spectra of 2.5CP/CN sample after 70 h continuous photocatalytic hydrogen production.

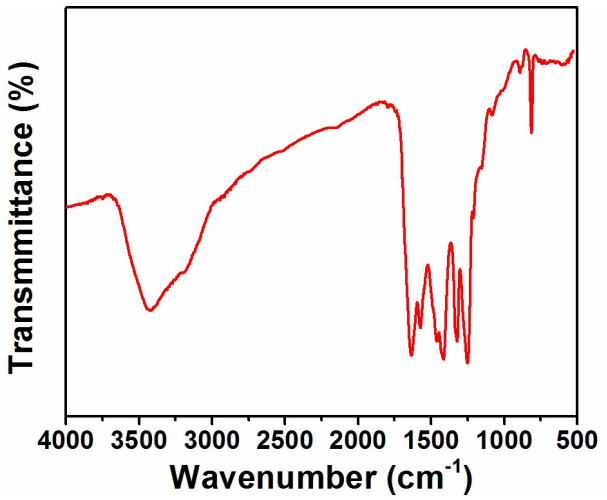

Fig. S20 FT-IR spectra of 2.5CP/CN sample after 70 h of continuous photocatalytic hydrogen production.

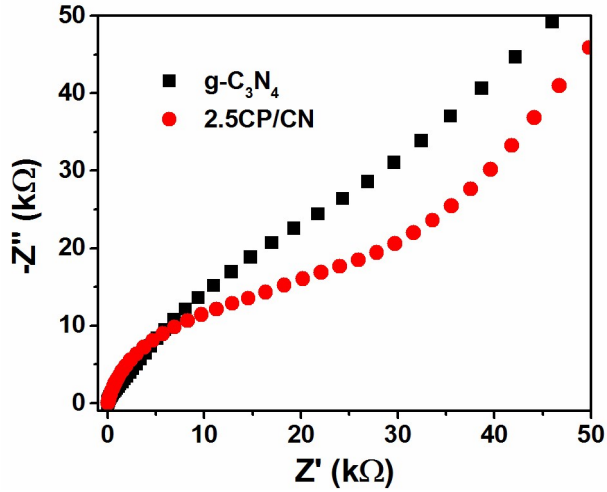

Fig. S21 EIS Nyquist plots of pure g-C_3N_4 and 2.5CP/CN samples.

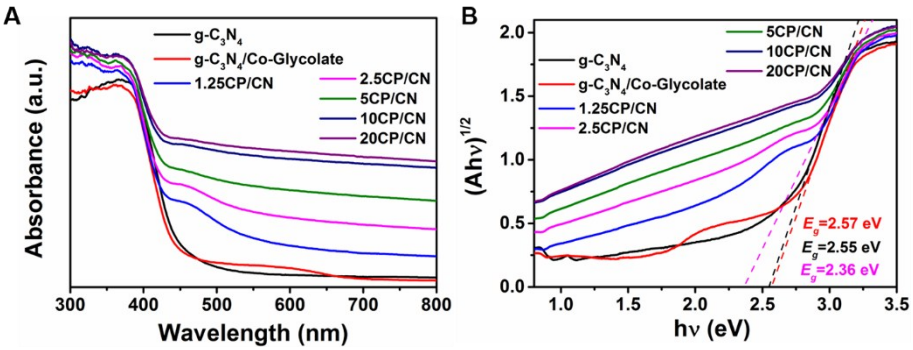

Fig. S22 (A) UV-vis diffuse reflectance spectra and (B) The Tauc plot of the pure g-C_3N_4, Co-Glycolate/g-C_3N_4, CoP/g-C_3N_4 composites with variable CoP mass contents (1.25, 2.5, 5, 10, 20 wt%).

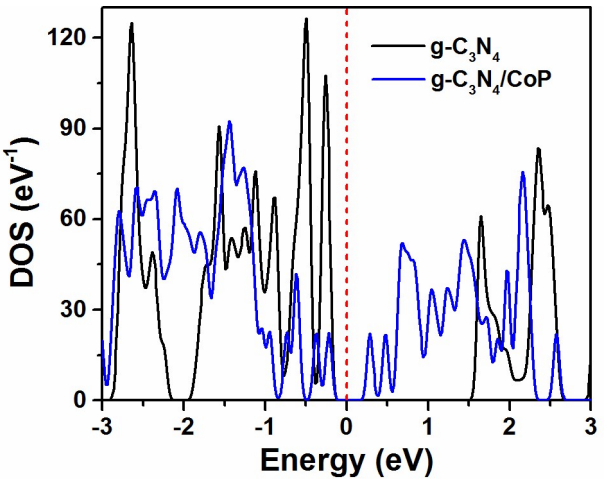

Fig. S23 Total density of states for pure g-C_3N_4 (black) and CoP/g-C_3N_4 (blue).

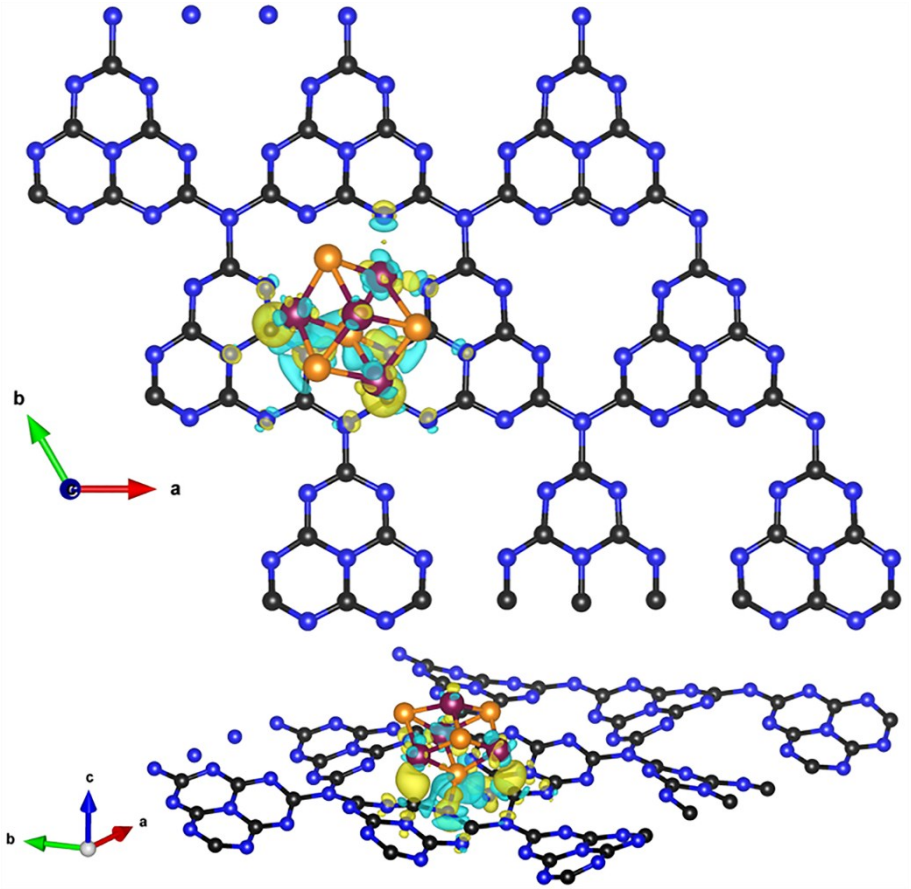

Fig. S24 Charge density difference isosurfaces of CoP/g-C_3N_4. The cyan region represents charge depletion, and the yellow region represents charge accumulation. The isosurface value is 0.05 e/Å^3. The blue, black, orange and violet spheres represent N, C, P and Co atoms, respectively.

Table S1 ICP results of the as-prepared CoP/g-C_3N_4 samples with variable CoP mass contents (1.25, 2.5, 5, 7.5 and 10 wt%).

Sample	Content (wt%)
1.25CP/CN	1.17
2.5CP/CN	2.44
5CP/CN	4.16
7.5CP/CN	6.05
10CP/CN	6.48

Table S2 ICP results of the as-prepared NiP_2/g-C_3N_4 samples with variable NiP_2 mass contents (6, 8 and 10 wt%).

Sample	Content (wt%)
6NP/CN	4.44
8NP/CN	6.37
10NP/CN	8.05

Table S3 ICP results of the as-prepared FeP/g-C_3N_4 samples with variable FeP mass contents (2, 6 and 10 wt%).

Sample	Content (wt%)
2FP/CN	2.52
6FP/CN	6.83
10FP/CN	8.87

Table S4 The hydrogen production activity of as-prepared FeP/g-C_3N_4 and NiP_2/g-C_3N_4 samples with variable FeP and NiP_2 mass contents.

Sample	H2 production (umol g^{-1} h^{-1})
6NP/CN	480.1
8NP/CN	655.8
10NP/CN	580.5
2FP/CN	129.1
6FP/CN	296.3
10FP/CN	194.6

Table S5 Comparison of photocatalytic H_2 evolution activities of the non-noble-metal cocatalyst modified g-C_3N_4 photocatalysts.

Catalyst	Synthetic method	Electron donor	Light source	H_2 production (umol g^{-1} h^{-1})	Ref.
Ni_2P/g-C_3N_4	Mixing the Ni salt, NaH_2PO_2, g-C_3N_4 and heating method	TEOA	≥ 420 nm	644	1
CoP/g-C_3N_4	Grinding method	TEOA	≥ 420 nm	474.4	2
$Ni_{12}P_5$/g-C_3N_4	Solution-phase self-assembly method	TEOA	≥ 420 nm	535.7	3
$Ni(OH)_2$/g-C_3N_4	Precipitation method	TEOA	≥ 400 nm	152	4
NiS/g-C_3N_4	Hydrothermal method	TEOA	≥ 420 nm	482	5
CoP/g-C_3N_4	**Reflowing-phosphorization method**	**TEOA**	**≥ 420 nm**	**956.8 (3 h) 861.3 (24 h) 783.8 (70 h)**	**Our work**

References

1. A. Indra, A. Acharjya, P.W. Menezes, C. Merschjann, D. Hollmann, M. Schwarze, M. Aktas, A. Friedrich, S. Lochbrunner, A. Thomas, M. Driess, Angew. Chem. 129 (2017) 1675-1679.
2. S.-S. Yi, J.-M. Yan, B.-R. Wulan, S.-J. Li, K.-H. Liu, Q. Jiang, Appl. Catal. B Environ. 200 (2017) 477-483.
3. D. Zeng, W.-J. Ong, H. Zheng, M. Wu, Y. Chen, D.-L. Peng, M.-Y. Han, J. Mater. Chem. A 5 (2017) 16171-16178.
4. J. Yu, S. Wang, B. Cheng, Z. Lin, F. Huang, Catal. Sci. Technol. 3 (2013) 1782-1789.
5. J. Hong, Y. Wang, Y. Wang, W. Zhang, R. Xu, ChemSusChem 6 (2013) 2263-2268.